Chapter 10

HR-MAS NMR Spectroscopy in Material Science

Todd M. Alam and Janelle E. Jenkins

Additional information is available at the end of the chapter

http://dx.doi.org/10.5772/48340

1. Introduction

In the early to mid-90's, NMR studies were being published that recognized the power of magic angle spinning (MAS) to increase resolution in materials that were not strictly solids by averaging differences in magnetic susceptibility and residual dipolar coupling inherent in these samples. The method of utilizing MAS for non-solid materials to produce liquid-like NMR lines was termed High-Resolution Magic Angle Spinning (HR-MAS). A few of the first HR-MAS examples included investigation of resins for combinatorial chemistry,[1] solvent swollen polystyrene gels,[2] and lipid systems.[3] Then in 1996, Maas *et al.* [4] advanced the field of HR-MAS NMR by adding a magnetic field gradient along the magic angle (see Figure 1). Like high resolution solution NMR, this gradient improved sensitivity and resolution with the ability to more easily select coherence pathways and by reducing indirect dimension (t_1) noise.[4]

There are currently commercially available HR-MAS probes with magic angle gradients from companies like Bruker BioSpin Corporation (Billerica, MA),[5] Agilent Technologies (Santa Clara, CA),[6] JEOL USA, Inc. (Peabody, MA),[7] and Doty Scientific, Inc. (Columbia, SC).[8] In addition to magic angle gradients, many of these probes also have a deuterium (^{2}H) lock channel, allowing improved ease of shimming and long term stability. With the emergence of commercially available probes, HR-MAS NMR has become more popular in the last few years, especially in the biological and biomedical fields. This popularity is mainly due to the heterogeneous nature of tissues and cells that are well suited for HR-MAS. Multiple HR-MAS NMR studies involving different tissue biopsies, like brain, kidney, liver, and muscle tissues for metabonomics studies, as well as identification of abnormal tissues (*i.e.* cancerous tissues) have been reported.[9-11] HR-MAS NMR has also been applied to the characterization of foodstuffs, including the assignment of metabolites in tomatoes and apples, the study of biopolymers in fruit cuticles, quantification of *n*-3 fatty acids content in different fish species, and tracking the chemistry of coffee beans during the

roasting process.[12, 13] These types of biological and foodstuff HR-MAS NMR investigations highlight the diverse range of information that can be obtained.

The application of HR-MAS NMR to material science was initially focused almost exclusively on the analysis of solid-phase (*i.e.* utilizing support resins) organic and peptide synthesis, or analysis of combinatorial solid-phase results. In these studies, the material was swollen in appropriate solvents such that the mobility of the attached ligands was increased, allowing high resolution NMR spectra to be obtained. The application of HR-MAS to solid state synthetic chemistry remains an active area of research, but will not be discussed in detail. The readers are encouraged to consult several very extensive reviews in this area.[14-16] In comparison to the numerous HR-MAS NMR studies on biological and solid-phase synthetic chemistry systems, there are fewer examples that focus on the use of this technique to material science. This chapter will review the application of HR-MAS NMR to a wide range of systems, including ceramics, zeolites, liquid crystals, ionic liquids, and surface modified nanoparticles.

1.1. How HR-MAS works

Materials that are crystalline or rigid solids (for example resins, ceramics, *etc.*) exhibit an extremely broad NMR signal due to extensive homo- and hetero-nuclear dipolar coupling, chemical shift anisotropy (CSA), and quadrupolar interactions. A variety of solid state NMR techniques have been developed to improve the resolution and sensitivity including the use of multiple pulse sequences, cross polarization, high power decoupling, multiple quantum NMR and fast MAS NMR. For example, solid state ^{1}H MAS NMR has found a number of applications in material characterization.[17] Even with these advances, solution-like NMR spectra are rarely realized for solid samples.

For samples that are in the liquid/solid classification, motional averaging will partially reduce or remove many of these broadening interactions. It is also possible to swell or plasticize a material to increase the local mobility, thereby reducing the magnitude of these interactions.[18] Even for liquid environments in a heterogeneous sample, differences in the magnetic susceptibility within the material can drastically reduce the observed resolution. For these types of dynamically averaged or susceptibility broadened systems, MAS even at moderate speeds will produce high resolution NMR spectra: this is the niche of HR-MAS NMR.

This improved resolution due to MAS arises because the Hamiltonians describing the dipolar, CSA and magnetic susceptibility interactions all contain an orientational component that scales as $(3\cos^2\theta-1)$, where θ is the angle between the rotor spinning axis and the magnetic field (Figure 1). When a sample is spun about an axis that is at the "magic angle" ($\theta = 54.7^{o}$) these interactions vanish. A simplistic schematic of a HR-MAS stator is pictured in Figure 1. As mentioned before, the main difference between a standard MAS stator and an HR-MAS stator is the magic angle gradient coil that can produce a gradient along the rotor spinning axis.

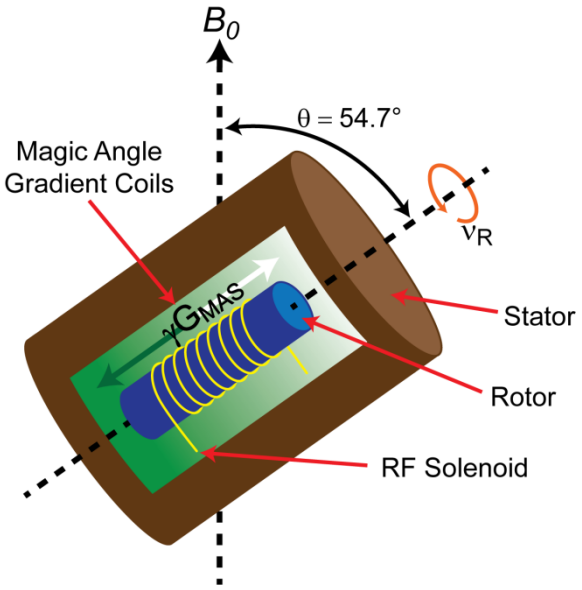

Figure 1. Schematic of a HR-MAS stator with a magic angle gradient along the rotor spinning axis.

For samples where residual dipolar interactions or differences in magnetic susceptibility are small, HR-MAS NMR reduces the observed line widths to be similar to those observed in solution high resolution NMR spectroscopy. For liquids adsorbed into/onto materials MAS speeds between 1 and 2 kHz may result in improved resolution, while for plasticized/swollen materials MAS speeds between 4 and 10 kHz may be necessary to obtain the desired resolution. Care must also be taken to ensure that the residual spinning sidebands (due to incomplete averaging) fall outside the spectral window of interest.

As an example of the enhanced resolution that can be achieved under HR-MAS two different swollen polymer systems are shown in Figure 2. These anion exchange membranes (AEM) operate in methanol solution, and readily adsorb significant amounts of water and methanol from the solution during use. Our group is interested in identifying the different chemical environments that these solvent molecules see within the membrane, as well as directly measuring the diffusion rates for these different species. Under static conditions, the water and methanol are not resolved in the NMR spectrum (Figure 2A, green). This lack of chemical shift resolution precludes any information about the local membrane environment being obtained. The broadening is caused by the magnetic susceptibility differences between the rigid AEM and the methanol solution. In this example, minimal MAS of ~750 Hz (Figure 2A, red) was sufficient to average the magnetic susceptibility allowing individual solvent environments to be easily observed. Increasing the spinning speed to 4 kHz removed the spinning side bands from the spectral region of interest, but did not dramatically increase the resolution of the solvent resonances. In this swollen AEM example, signals from the actual membrane are not observed at 4 kHz (only the swelling solvent is observed) indicating that the dipolar interactions present in the membrane remain much larger than

the MAS speed. Since the protons from the membrane are not readily observable, it provides a unique opportunity to further study the solvent behavior in the membrane without interference. Additional discussion of this system is presented in Section 2.1.1. The second example, involves the swelling of a polyButadiene-AcryloNitrile (pBAN) polymer in $CDCl_3$. Inspection of Figure 2B (green) shows that under static conditions this rather soft material produces a relatively unresolved NMR spectrum. Even after extensive solvent swelling, the NMR spectrum is essentially unchanged (Figure 2B, red). With HR-MAS (4 kHz spinning) the resolution is dramatically enhanced, enabling a more detailed analysis of the pBAN ^1H NMR spectra.

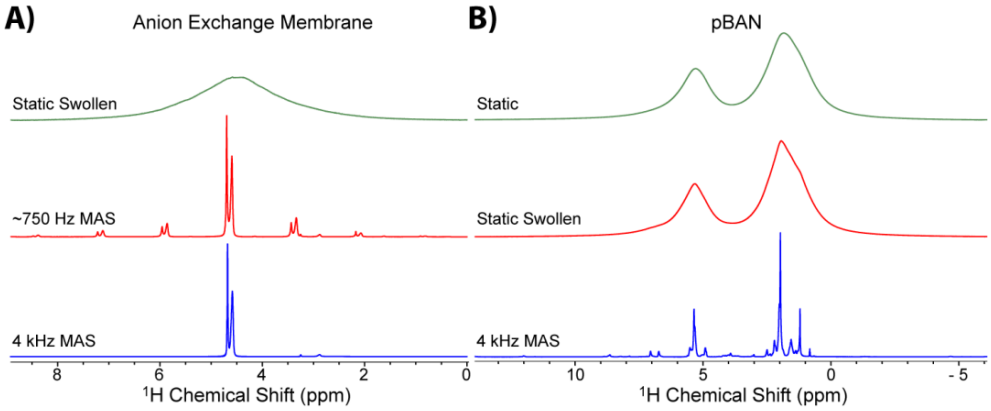

Figure 2. The improved resolution observed using ^1H HR-MAS NMR for the A) methanol swollen anion exchange membrane, and B) the $CDCl_3$ swollen pBAN (polyButadiene-AcryloNitrile) polymer.

With the dramatic increase in resolution observed utilizing HR-MAS, the arsenal of standard solution NMR techniques can be implemented for HR-MAS experiments, including solvent suppression, gradient-assisted sequences, and multiple-dimensional experiments. These can include INEPT (**I**nsensitive **N**uclei **E**nhanced by **P**olarization **T**ransfer), COSY (**CO**rrelation **S**pectroscop**Y**), NOESY (**N**uclear **O**verhauser **E**ffect **S**pectroscop**Y**), TOCSY (**TO**tal **C**orrelation **S**pectroscop**Y**), HETCOR (**HET**eronuclear **COR**relation), HMQC (**H**eteronuclear **M**ultiple **Q**uantum **C**oherence), and HMBC (**H**eteronuclear **M**ultiple **B**ond **C**orrelation) to name a few. As an example, a gradient-assisted 2D ^1H-^1H HR-MAS COSY NMR spectra for an ionic liquid adsorbed on an aluminum oxide membrane is shown in Figure 3. These types of correlation experiments could not be realized without the resolution afforded by HR-MAS. Additional discussion of this IL material is presented in Section 2.3.1.

It is also important to note that because anisotropic interactions (dipolar, CSA) are still present within these HR-MAS samples (though greatly reduced by molecular motion), it is also possible to apply some solid state NMR techniques during HR-MAS experiments. For example, to measure the residual homonuclear dipole-dipole interaction it is possible to incorporate a dipolar recoupling sequence to re-introduce this interaction under MAS. This

allows the incoherent NOE exchange process to be replaced by a coherent polarization transfer process. These types of HR-MAS recoupling experiments have been demonstrated using DQ COSY for solid state synthesis samples,[19] while our group has incorporated a radio frequency dipolar recoupling (RFDR) sequence into the standard NOESY experiment for lipid membranes, including the extension of this dipolar recoupling into a mixing period during ^{1}H-^{13}C Heteronuclear correlation experiments.[20]

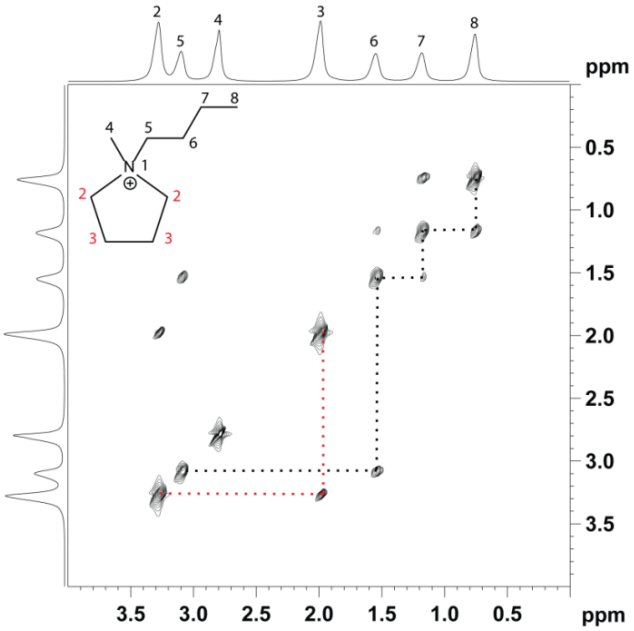

Figure 3. The gradient 2D ^{1}H HR-MAS NMR COSY spectrum for the ionic liquid $[MBPyrr]^{+}[TFSI]^{-}$ adsorbed into an inorganic aluminum oxide membrane. Even though the individual *J* couplings were not resolvable, these types of correlation experiments can still be realized under HR-MAS.

1.2. Experimental protocol and limitations

Many HR-MAS samples contain liquids or liquid-like materials. These samples require special care to prevent dehydration that can occur in a standard rotor with only a rotor cap. Various inserts are commercially available for packing of HR-MAS samples and can be seen in Figure 4. These inserts provide a tight seal to prevent dehydration or loss of solvent during MAS experiments. The inserts used generally depend on the sample size and need of the user. Examples of various insert options from Bruker BioSpin for a standard 4 mm rotor are shown in Figure 4. For ~12 μL samples, a Kel-F® bottom spacer (or a half drilled out rotor) and a top spacer with a seal screw can be utilized (Figure 4B, 4F and 4G). The top spacer insert (Figure 4F) contains a small hole in the top. When placed into the rotor at the properly gauged distance, any additional liquid will protrude through this hole. A Kimwipe® can then be utilized to remove this liquid, followed by using a small Kel-F®

screw to seal the insert (Figure 4B) and prevent dehydration. For ~50 μL volumes, a standard rotor can be utilized with the above top spacer and seal screw (Figure 4B, 4F, 4L). In addition to the spacers, a 30 μL disposable insert is also available (Figure 4I). The disposable Kel-F® inserts use a plug and screw cap to keep the sample well sealed (Figure 4B, 4H). The inserts are efficient if multiple samples need to be run, as samples can be packed into inserts and then easily placed into and removed from rotors, without having to wash the rotors between runs, and without having to own a large number of MAS rotors.

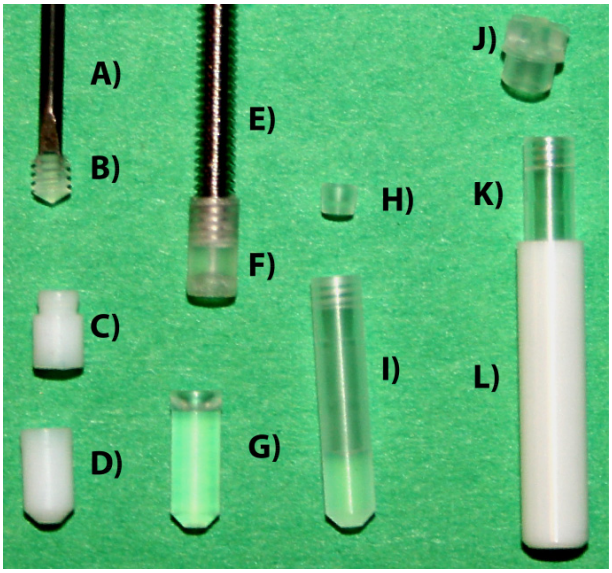

Figure 4. The tools and inserts used for HR-MAS NMR. These include A) the specialized tool for screw cap insertion, B) the sealing screw cap, C) the upper Teflon® insert, D) lower Teflon® insert for 30 μL volume, E) screw for insertion/extraction of top insert, F) top Kel-F® insert, G) bottom Kel-F® insert for 12 μL sample volume, H) plug for disposable insert, I) disposable 30 uL Kel-F® insert, J) 4 mm rotor cap, K) disposable inserted partially in a 4 mm rotor, L) 4 mm zirconia MAS rotor. All these parts are for the Bruker HR-MAS system, and may vary between vendors.

Temperature regulation is important in HR-MAS NMR for both sample purposes, and experimental reasons. The temperature of the bearing gas in many probes can be regulated to maintain a stable sample temperature; however, there is additional frictional heating that comes from spinning the rotor. To compensate for MAS related heating of the sample, the HR-MAS probe temperature should be calibrated at various MAS speeds and changes made to the temperature of the bearing gas to regulate the sample at the desired temperature. Temperature calibration of a HR-MAS probe has been discussed in literature.[21] This study utilized both methanol and glucose as NMR thermometers to determine the impact of MAS on temperature. Temperature changes measured at 2, 4, 6, and 8 kHz MAS where found to be 0.8 ± 0.1, 2.2 ± 0.1, 5.0 ± 0.1, and 7.9 ± 0.2 K in methanol and -0.3 ± 0.1, 1.2 ± 0.2, 3.0 ± 0.2, and 6.1 ± 0.1 K for glucose.[21]

Like all high resolution NMR techniques where resonances can be very narrow, it is important to be able to shim a sample to achieve the best possible resolution. Unlike standard high resolution NMR probes, the HR-MAS probes have the samples spinning at the magic angle, therefore the standard shimming protocols cannot be utilized. Instead, a combination of the standard shims must be used to address inhomogeneity of the B_0 field. By placing the probe so that the rotor is in the (x, z) plane in the laboratory frame, a combination of the laboratory shims can be used to express the Z shims along the magic angle. To obtain the equivalent response of a Z shim in standard shimming protocol, *i.e.* the Z shim along the magic angle (B_Z^{MAS}), the user needs to optimize a combination of the Z and X room temperature shims given by the linear relationship $B_Z^{MAS} = (1/\sqrt{3})B_Z^{LAB} - (\sqrt{2/3})B_X^{LAB}$. Likewise, the equivalent of a Z^2 shim is given by $B_{Z^2}^{MAS} = B_{(X^2-Y^2)}^{LAB} - 2\sqrt{2}B_{XZ}^{LAB}$ and the equivalent Z^3 shim is defined using $B_{Z^3}^{MAS} = -(2/3\sqrt{3})B_{Z^3}^{LAB} - (1/\sqrt{6})B_{XZ^2}^{LAB} + (5/\sqrt{3})B_{(X^2-Y^2)Z}^{LAB} - (5/3\sqrt{6})B_{X^3}^{LAB}$. The higher order Z shims map directly as $B_{Z^4}^{MAS} = -(7/18)B_{Z^4}^{LAB}$ and $B_{Z^5}^{MAS} = -(1/6\sqrt{3})B_{Z^5}^{LAB}$.[22] For the experimental examples discussed in this chapter, the authors typically only adjusted the shims up through $B_{Z^3}^{MAS}$. The Bruker Biospin Manual for High Resolution Magic Angle Spinning Spectroscopy points out that in theory shimming could be performed with just laboratory shims X, XZ,XZ^2, Z^4, and Z^5.[23] In reality, additional shims can be used to compensate for any inefficiency in the shim coil. A previous study has shown that once good shims are obtained, those shims can be utilized for samples with the same detection volume and position, for example the same sample size in the same type of rotor.[24] The shims should be independent of solvent because any susceptibility differences caused by solvent will be averaged out by MAS and does not affect the shims.[24] Piotto *et al.* also demonstrated shimming issues involved in systems containing water. In many cases, improved shims will be detected in an increase in lock signal. Deuterated water (HDO), however, has a strong chemical shift dependence on the temperature. When a sample spins, there can be a temperature gradient across the sample which can cause a portion of the HDO resonances to shift and broaden. If the probe is shimmed again based on the lock level from the water resonance, then any other signal in the spectra will most likely be deshimmed as those signals do not have as large of a chemical shift temperature dependence. With this in mind, Piotto *et al.* emphasize that shimming should be performed based on line shape, not lock level and attention should be taken when working with materials containing water.[24] More recently the MAGIC SHIMMING method has been described which utilizes a conventional homospoil gradient pulse to perform gradient shimming on MAS probes. This techniques does not require a gradient along the magic angle, and will reduce some of the trial and error presently inherent with manual shimming of HR-MAS probes.[25]

2. HR-MAS NMR spectroscopy in materials characterization

In this section a brief review of HR-MAS NMR studies involving the characterization of materials is presented. The majority of studies involved modified surfaces or surface interactions, and demonstrates the characterization need that HR-MAS NMR can fulfill.

2.1. Polymers

For rigid polymer materials the dipolar interactions are very large, leading to broadening of the NMR resonances, and can be characterized using standard solid state MAS NMR techniques. As noted before, these rigid polymers are not readily observed under HR-MAS conditions. For solvent swollen polymers the increased mobility of the polymer segments leads to a semi-solid regime where the moderate spinning speeds of HR-MAS are sufficient to produce high resolution NMR spectra. For example see the improved resolution observed for $CDCl_3$ swollen pBAN (Figure 2B). This ability to obtain spectra for mobile domains or components is the basis for the majority of HR-MAS polymer studies. A variety of different solvents are employed in combinatorial and solid phase synthesis, many of these with multiple ^1H resonances. In addition, there may be reasons to avoid having to dry the sample prior to introducing a deuterated solvent. In these cases, complicated solvent suppression techniques may be required.[26] It has been demonstrated that diffusion-filter HR-MAS spectra (see PFG discussion, Section 3.1) can provide suppression of solvent resonances based on differential diffusion behavior.[27]

One example of using HR-MAS NMR for characterizing polymer materials is the demonstration of the cyclic polyamide receptor threading onto the highly flexible polyethylene glycol (PEG) polymer chain attached to a polystyrene bead. Distinct PEG resonances for the threaded and non-threaded complexes could be easily resolved under HR-MAS conditions, while 2D NOESY spectra showed cross-peaks between the aromatic protons (δ ~ +8.87 ppm) of the rotaxane and the methylene protons (δ ~ +3.55 ppm) of the PEG polymer chain.[28] In another study, the complexation of Zn and Ru metalloporphyrins to beads functionalized with pyridyl ligands revealed that supermolecular interactions and changes in the dynamics are directly probed by HR-MAS techniques.[29]

The vulcanization of butadiene rubber (BR) with different curing systems has also been monitored by ^1H and ^{13}C HR-MAS NMR. This rubber is a very mobile system, with the increased resolution afforded by HR-MAS allowing the chemical identity of cross links to be determined, and revealing that α-substitution or addition depended on the disulfide cross-linkers employed.[30, 31] Other HR-MAS studies observed the impact of cross-linking in solvent swollen poly(amidoamine) polymers, the nature of water interactions in these same class of polymers, [32, 33] or the cross-linking performance in silicon-containing soybean-oil copolymers.[34] HR-MAS NMR has also been used to study the functionalization of poly hydroxyethyl methacrylate (HEMA) cryogels,[35] cyclomaltoheptaose polymers,[36] the synthesis of hyper-branched *bis* (hydroxymethyl) propionic acid (*bis*-MPA) polymers as a function of catalysts,[37] and polymers for nanoparticle stabilization.[38]

HR-MAS NMR has found use in investigation of porous polyalkylvinyl ether polymer particles being used for stationary phases in chromatographic applications. These measurements were performed using the same solvent as HPLC and allowed details about the polymer structure and mobility to be evaluated; these properties are expected to impact

the chromatographic process.[39] Interactions between solution molecules and the polymer component of HPLC stationary phases (C18, C30 and PEAA)[40] or the interaction with molecularly imprinted polymers [41] have also been investigated using HR-MAS NMR. These studies used saturation transfer difference pulse sequences to identify those molecules that were involved in binding to the larger stationary phase.

The NMR spectroscopic characterization of polymer degradation is commonly directed towards analysis of the small degradation fragments that are solvent soluble. By using HR-MAS NMR the hydrolytic degradation of the biodegradable photo-initiated cross linked poly(DL-lactide)-dimethacrylate (PDLLA) polymer network was directly monitored. Swelling these polymers in the solvent dimethyl sulfoxide (DMSO) and a combination of 1D and 2D (COSY, NOESY) experiments allowed the different signals in the PDLLA chain to be identified. Degradation in a base was shown to occur through hydrolysis of the ester bonds within the poly(lactide) segment.[42] HR-MAS has also been used to study the role of partial hydrolysis in controlling the composition of hydrophobic polyacrylamide gels.[43]

2.1.1. Example: HR-MAS NMR investigations of anion exchange membranes

The increased resolution achieved with ^{1}H HR-MAS on the solvent swollen anion exchange membrane (AEM) was demonstrated in Figure 2. Due to differences in the magnetic susceptibility between the swelling solution and the polymer membrane, the water and methanol resonances were not resolved under static conditions. Under HR-MAS four distinct NMR resonances were observed for the solvent species; two water resonances and two methanol resonances. Based on line widths and PFG HR-MAS diffusion measurements (Section 3.2.1) the higher ppm shifted water and methanol were assigned to bulk (or free) methanol or water within the membrane, while the lower ppm shifted water and methanol resonances exhibit slower diffusion rates and were assigned to water or methanol associated (bound) within the membrane. The increased resolution obtained under HR-MAS was further exploited to explore the interchange of water and methanol between the different binding environments within the AEM using 2D HR-MAS NMR NOESY exchange experiments (Figure 5). At short mixing times (1 ms) no correlations were observed between any of the resonances. With increasing mixing time (> 10 ms), cross peaks were observed between free water and membrane-associated water, plus cross peaks between free methanol and membrane-associated methanol, resulting from physical exchange of water (red dashed lines) or methanol (red dashed lines) between the free and unbound environments. With long mixing times (> 200 ms), NOE correlation between methanol and water were observed (green dashed line), and result from through space NOE magnetization exchange (not physical spatial exchange). Interestingly, these NOE correlations were only observed between associated water and associated methanol, as well as free water and free methanol, supporting the assignment and indicating that the spatial contact of water and methanol is maintained in these associate membrane environments. Additional exchange studies are ongoing.

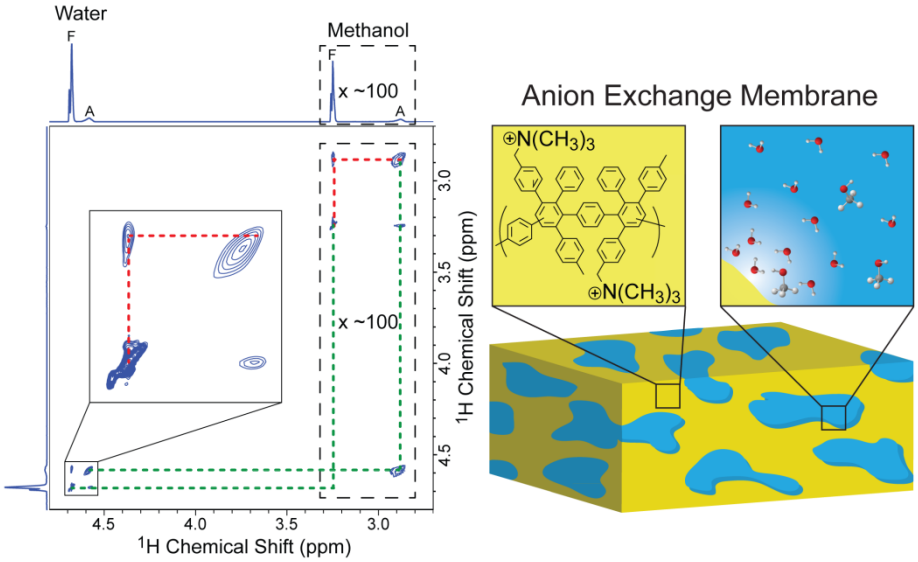

Figure 5. 2D ^{1}H HR-MAS NMR NOESY spectrum (500 ms mixing time) of an anion exchange membrane swollen in a 1N methanol solution. The increased spectral resolution obtained for the swelling solvent made it possible to detect exchange between free and associated water and between free and associated methanol (red dashed lines), as well as NOE magnetization exchange between free water and methanol and associated water and methanol (green dashed lines).

2.2. Ceramics, zeolites, catalysts surfaces and composites

Due to the rigid or crystalline nature of ceramics, zeolites, catalysts or inorganic/organic composites, solid state MAS NMR spectroscopy remains the dominant NMR characterization method, and can involve a range of nuclei and multi-pulse NMR techniques. In contrast, the limited number of HR-MAS NMR studies is directed towards the investigation of gas/solid adsorption or intercalation within these materials. For example, the degradation of the pesticide diethyl parathion and the chemical warfare agent (CWA) simulant diisopropyl fluorophosphates in functionalized montmorillonite clay using ^{31}P HR-MAS NMR has been reported. The HR-MAS removed susceptibility effects present from the clay material, and allowed a direct measure of the decomposition kinetics. The adsorption of organosilanes on the $MgCl_2$ in Ziegler-Natta catalysts has been investigated using ^{1}H HR-MAS, and demonstrates differential binding (differential mobility) to the Mg surface with changing surface coverage and as a function of the degree of saturation in the Mg coordination sites.[44]The polymer mobility in the condensed sol-gels produced from organosilanes and phenyl siloxanes was also evaluated.[45]

2.3. Ionic liquids and liquid crystals

HR-MAS NMR should be an ideal tool for the characterization of ionic liquids (ILs) and liquid crystals (LC) due to the high viscosities commonly encountered in ILs, and the

thermal- or concentration-induced ordering transitions of LCs. Ionic liquids are interesting compounds, and continue to be used for a wide range of material science applications. ILs are used as liquid electrolytes in energy storage and production devices, solvents for CO_2 capture and green chemistry, solutions for biomass processing, nanostructured synthesis and solvents for catalysis reactions. For many of these applications room temperature ionic liquids (RTIL) are utilized as neat solutions without another solvent. Strong attractions between the IL cation and anion component may lead to the formation of important structural motifs that could be missed or changed with the introduction of a solvent. For NMR characterization, solvent-IL interactions may also mask subtle changes in the chemical shift produced by other molecular interactions of interest. In the case of ILs, it is now recognized that HR-MAS NMR provides a powerful tool for the characterization of these systems.

One of the earliest reports involving HR-MAS NMR of ILs studied silica-immobilized ILs suspended in DMSO,[46] which produced nearly liquid-like resolution. In this same study, they were also able to obtain 2D ^{1}H-^{13}C HR-MAS NMR HMQC spectra of these attached ILs. Another study explored the use of ILs as a solvent or chemical reaction media. The standard solution NMR of compounds dissolved in these ILs suffered from low resolution, produced by the high viscosities of the ILs, dynamic range issues due to the lack of deuterated ILs, and concerns about chemical shift referencing due to the high magnetic susceptibility of ILs. To demonstrate the capabilities of HR-MAS NMR, Rencurosi and co-workers[47] dissolved *para*-methoxy benzyl acetate and a glucopyranoside in a series of different ILs. Even at moderate spinning speeds there was significant improvement in resolution, and the chemical shift referencing became consistent with that observed in solution NMR using traditional deuterated solvents. In addition, they were able to follow acetylation of *para*-methoxybenzyl alcohol directly in the ILs. The increased resolution inherent in this technique was also important for investigations of CO_2 interactions with imidazolium based ILs using ^{13}C HR-MAS NMR.[48] ^{1}H HR-MAS NMR has also been used to probe the interaction of the RTIL *N*-methylimidazolium chloride ($[Hmim]^{+}Cl^{-}$) with the silica surface of Aerosil. This adsorption was monitored through changes in chemical shift with increased IL loading and Cl^{-} salt concentration. Based on the magnitude of the chemical shift variations, the interaction was found to preferentially involve the H(2) position of $Hmim^{+}$, and was a physisorption versus a chemisorption process.[49] In another study, the dynamics of IL's confined in monolithic silica ionogels were followed by ^{1}H HR-MAS NMR and relaxation experiments, and demonstrated that the IL maintained liquid like behavior with very little reduction in motions even as the pore size diminished from 12 nm to 1.5 nm.[50] Surprisingly, only a single ^{1}H HR-MAS NMR diffusion study of a non-biological LC material confined in nanopores has been reported.[51]

2.3.1. Example: HR-MAS NMR investigation of ionic liquids on surfaces

While many RTILs are "liquids" at room temperature, they can be highly viscous, making standard solution NMR analysis on the neat ILs challenging (as noted above). In our

laboratory, a novel series of quaternary ammonium and cyclic pyrrolidinium RTIL have been studied using different NMR techniques. This includes pulse field gradient (PFG) NMR to measure diffusion and ^{14}N NMR relaxation experiments to determine IL molecular reorientation times.[52] More recently, we have explored using ^{1}H HR-MAS NMR to characterize the interactions between IL and metal oxide surfaces. Figure 6A shows the ^{1}H HR-MAS NMR spectra of the neat ionic liquid, *N*-methyl-*N*-(n-butyl) pyrrolidinium bis(trifluoromethanesufonyl) imide ([MBPyrr]$^{+}$[TFSI]$^{-}$). The changes in the NMR spectrum for the neat solution under static conditions (top) and under MAS conditions (bottom) demonstrate the simple resolution enhancing properties of HR-MAS (previously discussed in Section 1.1). The static NMR spectrum revealed distorted line shapes reflecting poor magnetic field homogeneity across the sample volume, along with broadening (FWHM ~ 115 Hz) due to differences in local magnetic susceptibility within the sample. The broad line width is commonly encountered when working with highly viscous RTIL that are not dissolved into solvents. Increasing the temperature (within the limitations of the instrumentation) will improve the resolution for these RTIL, but may not be desirable in some instances. Not surprisingly, even slow spinning (~1 kHz) of the neat RTIL provides an immediate improvement in the resolution. For the ([MBPyrr]$^{+}$[TFSI]$^{-}$) example, the line width are reduced to ~ 3 Hz (~40 fold reduction), such that small ^{1}H-^{1}H spin-spin *J* coupling are clearly resolved (Figure 6A, bottom).

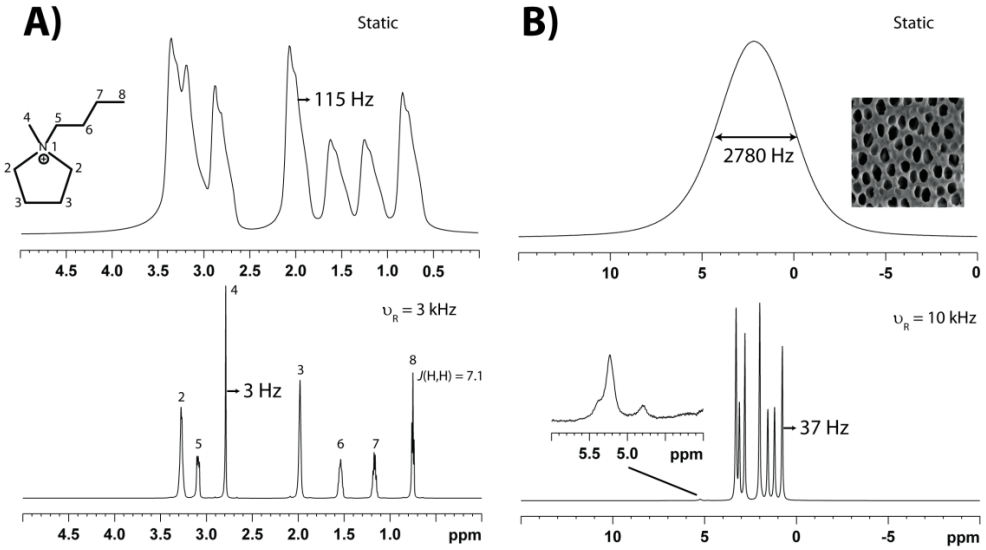

Figure 6. The ^{1}H HR-MAS NMR of the ionic liquid [MBPyrr]$^{+}$TFSI^{-} at 298K as a A) neat liquid and B) adsorbed (20 wt%) into an aluminum oxide ANOPORE inorganic membranes (200 nm pore diameter). The spectra in the top portion of each figure were obtained under static conditions, with the spectra in the bottom portions of each figure obtained under MAS conditions.

The loss of resolution is even more dramatic when $[MBPyrr]^+[TFSI]^-$ is adsorbed into the small pores (200 nm) of an inorganic aluminum oxide membrane. The ^1H NMR spectrum of the static sample is now a broad (~2780 Hz) featureless line providing no chemical shift resolution. Under HR-MAS the individual ^1H resonances become resolved, with a line width on the order of 37 Hz. While the individual *J* couplings are no longer resolved as they were in the neat IL case, the resolved chemical shifts allow one to compare directly with the neat IL. In the adsorbed $[MBPyrr]^+[TFSI]^-$, the *n*-butyl methyl group protons (H-8) and the ring methylene protons (H-3) show a very small chemical shift change ($\Delta\delta$ = 0.007 ppm) due to adsorption with the ANOPORE membrane. In contrast the methyl group (H-4) and the *n*-butyl methylene protons (H-5) reveal an asymmetric line shape with chemical shift variations ranging from $\Delta\delta$ = +0.01 to +0.02 ppm. This result suggests that while the adsorption process is weak, it occurs preferentially through the IL N^+ with the surface. The ability to resolve such small differences under HR-MAS NMR is important in identifying these surface interactions.

Even though the ^1H HR-MAS NMR spectra for the surface adsorbed $[MBPyrr]^+[TFSI]^-$ does not reveal resolvable *J* coupling, it is still possible to obtain a 2D COSY spectrum for this material, as shown in Figure 3. This correlation experiment immediately confirms the chemical shift assignments for the neat IL sample, and clarifies differences seen for the IL dissolved in a solvent. The 2D ^1H HR-MAS NOESY NMR spectra for the IL $[MBPyrr]^+[TFSI]^-$ adsorbed into the ANAPORE membrane is shown in Figure 7. Interestingly there are numerous cross peaks observed even at moderate mixing times, reminiscent of the liquid-ordered phase observed in lipid bilayers (For example see Ref. [20, 53, 54]). These through-space correlations are stronger than those observed in the neat IL (not shown), and suggest that an increase in the dipolar-dipolar interactions is occurring for the surface adsorbed species. This argues that local motions have become reduced for the adsorbed species. There are also some missing or weak correlations (dashed circle) implying distinct conformations present for the *n*-butane chain on the adsorbed species. Also of interest is the appearance of new chemical environments for the adsorbed IL. This includes a weak resonance at δ = +4.8 ppm which is assigned to residual water, but shows no correlations with the IL. There are two additional ^1H environments at δ = +5.2 and +5.3 ppm, which are attributed to additional surface water species on the aluminum oxide surface. The environment at δ = +5.2 ppm shows a through space NOE correlation with a new resonance near 2 ppm. This small resonance is buried under the shoulder of the dominant methylene (H-2) resonance and has not been presently assigned. These types of correlation experiments demonstrate the capabilities and information that can be obtained from HR-MAS studies of ILs, and suggest future efforts along these lines are warranted.

2.4. Surface modified nanoparticles

HR-MAS NMR studies of surface modified nanoparticles (NP) are closely related to those of the polymer resin studies mentioned in the previous sections, with accurate

characterization of the surface-attached ligands being the primary objective. For NPs the solvent plays the role of suspending or dispersing the material, in contrast to the role of swelling that the solvent plays in analysis of resins. For HR-MAS NMR studies of NPs, the optimal solvent provides both high solubility, and good dispersion (prevents aggregation) of the NPs.

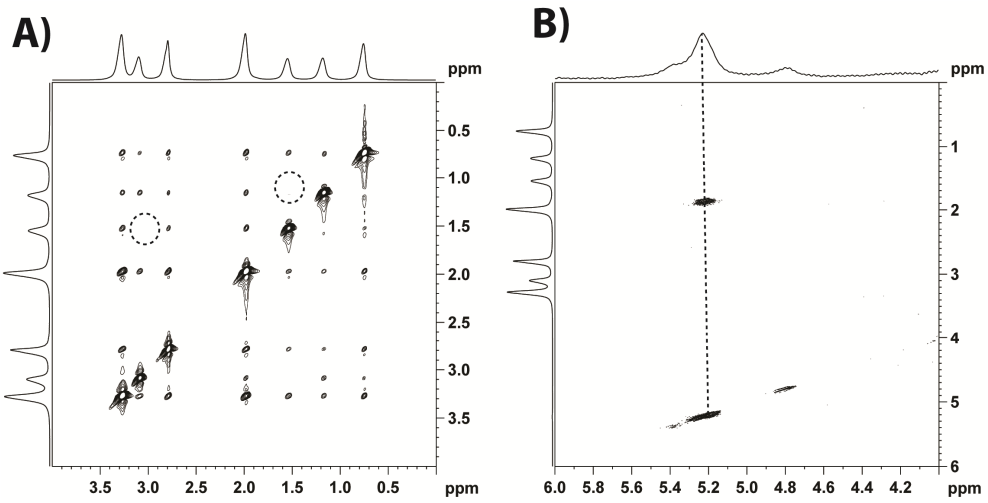

Figure 7. The 2D ^{1}H HR-MAS NOESY NMR correlation spectra for the ionic liquid $[MBPyrr]^{+}[TFSI]^{-}$ adsorbed into an inorganic aluminum oxide membrane (pore size 200 nm). The spectrum in A) shows numerous through space correlation between the protons of the IL, while B) shows the spectral expansion for the water and surface associate-water species and corresponding NOE correlations.

HR-MAS NMR studies of surface modified NPs include the 1D and 2D ^{1}H NMR investigation of modified gold (Au) NPs using a wide range of high resolution correlation experiments: COSY, TOCSY and HMQC.[55] This revealed that the relative signal sensitivity (intensity) depends on the distance between the detected ^{1}H and the surface of the Au NP. This distance correlation is either a function of reduced local dynamics, or spin-spin T_2 relaxation effects governed by the Au surface. Another study involved the active molecular compounds Aloin A and Aloesin extracted from the leaf of Cape Aloe, and was able to show how these compounds selectively stabilize Au NPs preferentially through the glucose component.[56] HR-MAS NMR has also been used to identify the binding motif of peptides on the Au NP surface.[57] While HR-MAS NMR is typically employed to overcome anisotropy of magnetic susceptibility or residual dipolar interactions, Poito and co-workers[58, 59] have reported an interesting set of experiments that demonstrated HR-MAS can be employed to overcome paramagnetic effects present in iron oxide NPs. Through a careful analysis of these iron oxide systems, the surface structure and ligand binding (chelation) configuration was determined, and in several cases were quite different from the standard single point attachment proposed by others.[58]

^{1}H HR-MAS NMR has also been used to look at the surface modification in polymer based NPs, including the monitoring of multiple synthetic steps employed during the peptide-surface modification of poly(vinylidene fluoride) (PVDF) nanoparticles,[60] or the surface modification of Dendron based NPs.[61] Polystyrene embedded silver clusters produced by a thermolysis reactions have also been characterized using HR-MAS NMR.[62]

2.5. Surface immobilized linkers and catalysts and chiral stationary phases

HR-MAS NMR spectroscopy has also been extensively used in investigating the mobility of linkers and catalysts attached to other materials, including ^{1}H and ^{31}P HR-MAS NMR studies of phosphine, bisphosphinoamine linkers and corresponding metal catalysts.[63-66] These investigations demonstrate very nicely that the surface mobility as probed by HR-MAS is strongly dependent on the swelling solvent employed in the studies.[67] The grafting of organotin catalysts to polystyrene for the tranesterification reaction between ethyl acetate and *n*-octanol or the ring-opening polymerization of ε-caprolactone has been followed by both 1D and 2D ^{1}H, ^{13}C and ^{119}Sn HR-MAS NMR.[68-70] While the catalytic activity of the attached tin was unchanged following numerous cycles, the NMR revealed there was actually a change in the liquid-solid interface with a reduction in the mobility of the undecyltin trichloride catalyst at the resin surface. For experiments with rapid catalytic turnover rate there was a reduction in performance. This reduction in activity was reversible with solvent extraction, and was confirmed by HR-MAS to involve the change of the Sn environment back to the original state.[69] The use of ^{119}Sn HR-MAS NMR has also been demonstrated to provide a quantitative measure of the tin loading in supporting catalysts.[71] This HR-MAS NMR study was also the first to incorporate the ERETIC (*e*lectronic *re*ference *t*o access *i*n vivo *c*oncentration) method.

HR-MAS NMR techniques have been used to characterize the surfaces of silica and polystyrene particles modified with chiral agents that allow identification of different enantiomers. In one study the NMR was able to probe regiochemistry of the surface chemistry, along with monitoring the stability against decomposition of the polystyrene resins.[72] Another investigation used 2D transfer NOESY NMR experiments to evaluate the stereoselective binding of molecules to the chiral stationary phase based on the negative cross-peaks associated with the transfer NOE effect.[73]

2.6. Soil and humic materials

While standard solid state MAS NMR techniques have become common in the investigations of humic, soil and coal materials, the implementation of HR-MAS techniques for these materials has been more limited. The ability of HR-MAS to identify different motional regimes has proven powerful in the elucidation of the chemistry at water/soil interfaces.[74-79] These NMR studies show that at this interface fatty acids, aliphatic esters and alcohols are the prominent species, and that aromatic functional groups are protected by hydrophobic regions and are not directly accessible to the penetrating water,[74] while surface polymethylene groups may control the sorption properties of organo-clay

complexes.[76, 80] These types of studies have been extended to three-dimensional (3D) HMQC-TOCSY to further increase the resolution of the highly overlapping spectra from humic materials.[81]

3. PFG HR-MAS NMR to measure diffusion in materials characterization

Modern HR-MAS probes include a gradient coil that can produce a magnetic gradient along the long axis of the MAS rotor which is set at the magic angle ($\theta = 54.7^{o}$). Standard MAS probes have also been combined with micro-imaging gradient systems in which gradient coils wrapped around the stator were not employed, but instead rely on imaging gradients that were external to the probe. [82] This is not the common configuration, and has been replaced by significant development efforts from the instrumental vendors involving the integration of gradients directly into the HR-MAS probes. With the gradient coil along the magic angle pulsed field gradient (PFG) experiments can be performed under MAS conditions. Fortuitously, enhanced T_2 times are generally observed under MAS allowing PFG experiments with longer diffusion times to be implemented than would have been accessible with static conditions.

During the PFG diffusion experiments, the application of a gradient "tags" a spin with a phase that is related to its spatial position. Figure 8A provides a pictorial representation of the dephasing of spins around the magic angle caused by the magic angle gradient. If the position of the spin does not change during the diffusion period (Δ), this dephasing is refocused and the original signal intensity (S_0) is recovered. If on the other hand the spin changes spatial position (diffuses) during Δ, the dephasing for that spin is not refocused, and the signal intensity decreases. The loss in signal intensity with increasing gradient strength is related to the self-diffusion rate with the classic Stejskal-Tanner equation:

$$\frac{S}{S_0} = e^{-\gamma^2 g^2 \delta^2 \left(\Delta - \frac{\delta}{3}\right) D} \tag{1}$$

where S is the experimental amplitude of the signal, γ is the gyro magnetic ratio, g is the gradient strength, δ is the gradient pulse length, Δ is the diffusion time, and the D is the diffusion constant.[83] By fitting this decay the diffusion constant can be determined. Figure 8B shows an example of the signal intensity loss observed during diffusion experiments for the different two water environments present in swollen AEM with increasing gradient strength.

PFG diffusion HR-MAS NMR experiments can also be used to obtain diffusion-filtered NMR spectra through the separation of different motional regimes present in complex mixtures. This filtering is accomplished by selecting Δ times where the signal intensity (Eqn. 1) for the fast diffusing components has been highly attenuated, while the slow diffusing components have significant signal intensity remaining. Practical aspects of diffusion measurements using HR-MAS have been previously discussed by Viel *et al.* [84] A significant finding from this study was that sample volume played a role in the reliability of diffusion rates measured. It was shown that small volumes (~12μL) exhibit reproducible

diffusion rates, while larger volumes (~50μL, a full 4 mm rotor) produced inconsistent or unreliable data.

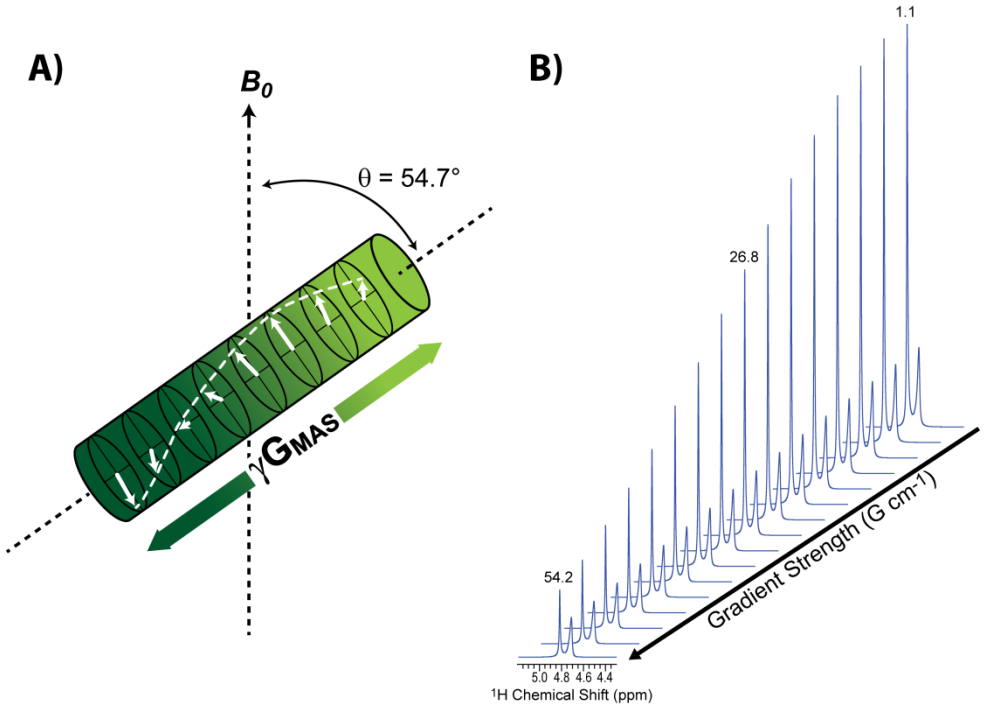

Figure 8. A) Pictorial representation of the gradient produced along the magic angle of the rotor. B) The decay of two different water signals found in a 1N methanol solution of an AEM membrane with increasing gradient strength. Gradient strength values (G/cm) are shown above the stack plot.

Three commonly used PFG diffusion pulse sequences are shown in Figure 9. The basic spin-echo diffusion sequences is depicted in Figure 9A, but is limited by loss of signal intensity due to spin-spin T_2 relaxation during the diffusion period Δ. Two variations of the stimulated echo (STE) sequence are shown in Figure 9B and 9C, and in this case spin-lattice T_1 relaxation is occurring during the diffusion Δ period. For most materials T_1 values are longer than T_1 making these STE sequences the preferred choice for material analysis. It should be noted that all of the gradient pulses in these sequences are trapezoidal shaped to compensate for the inability of instrumentation to generate perfect rectangular gradients. Shaped pulses, like sine or trapezoidal shapes, are used to produce experimentally reproducible gradient pulses. The PFG stimulated echo with dipolar gradients and spoil gradient, depicted in Figure 9B, is beneficial for the use with many HR-MAS samples which exhibit differences in magnetic susceptibility across the sample.[85, 86] The PFG stimulated echo in Figure 9C has an additional delay to the PFG stimulated echo in Figure 9B that is utilized to address eddy currents within the sample.[87]

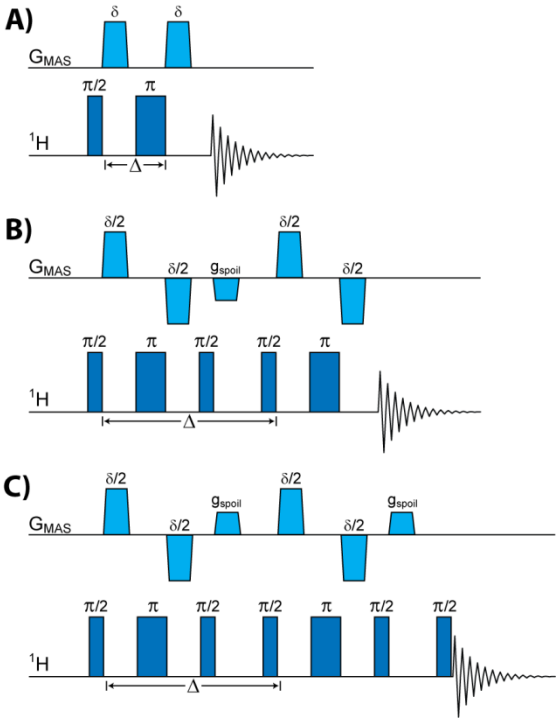

Figure 9. Diffusion pulse sequences. Pulse Field Gradient (PFG) A) Spin-Echo, B) PFG Stimulated Echo with dipolar gradients and spoil gradient based on Cotts *el al.* 13-interval sequence[85], and C) PFG Stimulated Echo with dipolar gradients and spoil gradient with an additional eddy current delay. GMAS indicates that the gradient is applied along the magic angle.

3.1. Diffusion in zeolites, nanoparticles and liquid crystals

As noted for other material studies, heterogeneities in the magnetic susceptibility or restricted molecular motions within zeolite crystallites lead to broadening of the NMR signal, such that resolution of individual species in mixtures becomes difficult. HR-MAS NMR resolves this issue, and has led to the utilization of PFG NMR diffusion experiments on organic mixtures in zeolites. This technique has been used to study the diffusion of *n*-butane in silicalite-1,[88] ethane, water and benzene mixtures adsorbed to the zeolite NaX,[89] acetone-*n*-alkane (C_6 to C_9) mixtures in nanoporous silica,[90] or mixtures of *n*-butane and *iso*-butane adsorbed in MFI zeolite. The increased resolution afforded by these PFG HR-MAS studies on mixtures reveal the obstructive influence of the isopropyl molecules or bulky benzene on the diffusion of other molecular species, [89, 91] and that the creation of acetone-alkane complexes greatly impacts the observed diffusion properties.[90]

PFG HR-MAS NMR has also been used to obtain 2D DOSY (**D**iffusion **O**rdered **S**pectroscop**Y**) spectra of surface modified iron oxide NPs. These results were able to distinguish between NP-bound and free ligands in these materials.[58] These types of PFG

HR-MAS NMR experiments should prove useful in understanding the surface-ligand dynamics present in modified NPs.

Diffusion experiments using HR-MAS NMR has also been found useful in the analysis of transport properties in lipid membranes.[92-94] Due to the anisotropic molecular reorientation of these liquid crystalline (LC) systems, significant dipolar coupling remains, leading to broad lines and short relaxation times. However dipolar coupling can be reduced through the use of MAS. Surprisingly, the use of PFG HR-MAS NMR for non-biological LCs is more limited, with the single investigation of local molecular dynamics of the thermotropic LC 4'-pentyl-4-cyanobiphenyl (5CB) confined in Bioran glasses with pore diameters of 30 nm and 200 nm being reported. By utilizing PFG techniques it was possible to measure the diffusion constants as a function of temperature through the isotropization temperature of the liquid crystal, thus demonstrating that for this case there is only a minor reduction in the diffusion rates with molecular confinement.[51]

3.2. Diffusion in polymers

There is extensive literature on the use of PFG NMR to measure diffusion of polymer solutions and melts, along with PFG diffusion measurements of different species adsorbed into polymers, including gases, water, organic solvents and electrolytes. There have been a limited number of examples where the improved resolution afforded by HR-MAS NMR was coupled with PFG. This work includes the development of diffusion filtered HR-MAS NMR techniques to study the gelation process of super-molecular gels,[95] along with a combination diffusion-filtering and a spin-echo enhanced (T_2 –filtered) experiment on DMF-swollen resins.[96] These techniques allowed the identification of free and surface bound molecules, while eliminating the signal from the immobile bulk resin matrix. In complex mixtures there may be future avenues for HR-MAS to resolve subtle differences in the local chemical environments as demonstrated in the following example.

3.2.1. Example of HR-MAS diffusion in anion exchange membranes

As discussed in Section 2.1.1, four distinct resonances were observed in the 1D ^{1}H HR-MAS NMR spectra of AEM polymers swollen in a 1N methanol solution. In Figure 10A, NMR spectra for three AEM polymers with different ion exchange capacities (IEC) are shown. Two resonances were observed for both water and methanol, and were assigned to free (F) and membrane-associated (A) environments. From this HR-MAS data it is easy to see that there is a correlation between chemical shift of the associated species and the IEC of the membrane, with both the associated water and methanol resonance shifting to lower ppm with decreasing IEC. This decrease in chemical shift is most likely due to a change in hydrogen bonding between the solvent components and the membrane, reflecting how strongly the solvent molecules are associated with the membrane. Recall that the resolution of these individual environments was not observable in the static NMR spectra (Figure 2A). Using ^{1}H HR-MAS PFG diffusion experiments, the self-diffusion constants were obtained for each of these four different environments, which were not accessible from the static data.

Because the ^{1}H signal for the AEM membrane is not readily observable under HR-MAS conditions, the diffusion rates obtained for the resolved solvent resonances were not biased by the polymer membrane. Figure 10B shows the signal decay for the associate methanol environment as a function of gradient strength for the three different IEC levels. The magic angle gradients were used to perform diffusion measurements utilizing a PFG Stimulated Echo with dipolar gradients and spoil gradient with a Δ=100ms (Figure 9B). The signal decay shows that there is a correlation between diffusion rate and IEC, exhibiting a faster diffusion rate with increasing IEC values. A more detailed analysis of this work is forth coming, but this example demonstrates the power of combining HR-MAS and PFG diffusion experiments.

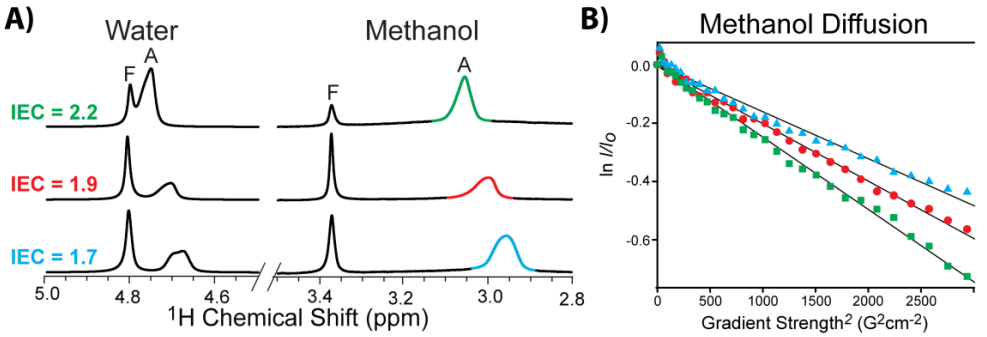

Figure 10. A) ^{1}H HR-MAS NMR spectra with the assigned free [F] and associated [A] water and methanol environments. B) The diffusion rates for the associated methanol in three different anion exchange membranes with varying ion exchange capacity (IEC) values. The colored peaks in the ^{1}H HR-MAS NMR spectra correlate to the colored symbols in the diffusion plot of the associated methanol peak of IEC = 2.2 (■), 1.9 (●), and 1.7 mequiv/g (▲).

4. Conclusions

The application of HR-MAS NMR to the characterization of materials or material interfaces that exist in the semi-solid range has been demonstrated. A wide variety of different material systems have been explored, showing that this technique can provide resolution and dynamic information where standard solution or solid state NMR techniques were unsuccessful. HR-MAS NMR is a powerful tool for the detailed characterization of modified surfaces and surface adsorbed species. This technique also provides a direct probe of differences in local mobility as reflected by line width variations. Through the combination of the enhanced resolution afforded by HR-MAS with pulse field gradient (PFG) capabilities, selective filtering and diffusion measurements of complex heterogeneous materials can also be realized. The ability to resolve and obtain diffusion rates for multiple environments in materials will prove beneficial for understanding the diffusion process in mixed chemical systems. While HR-MAS NMR is considered a mature, relatively routine technique, the application to the materials field is expected to continue being an active area of development. It is hoped that this review will encourage researchers to explore the application of HR-MAS NMR techniques to their different material systems.

Author details

Todd M. Alam* and Janelle E. Jenkins
Sandia National Laboratories, Department of
Nanostructured and Electronic Materials, Albuquerque, NM, USA

Acknowledgement

Sandia National Laboratories is a multi-program laboratory managed and operated by Sandia Corporation, a wholly owned subsidiary of Lockheed Martin Corporation, for the U.S. Department of Energy's National Nuclear Security Administration under contract DE-AC04-94AL85000. The authors would like to acknowledge Michael Hibbs (Sandia) for providing the anion exchange membranes.

5. References

[1] Sarkar S. K., Garigipati R. S., Adams J. L., Keifer P. A. (1996) An NMR Method To Identify Nondestructively Chemical Compounds Bound to a Single Solid-Phase-Synthesis Bead for Combinitorial Chemistry Applications, *J. Am. Chem. Soc.* 118:2305-2306.

[2] Stöver H. D. H., Frèchet J. M. J. (1991) NMR Characterization of Cross-Linked Polystyrene Gels, *Macromolecules* 24:883-888.

[3] Gross J. D., Costa P. R., Dubacq J.-P., Warschawski D. E., Lirsac P.-N., Devaux P. F., Griffin R. G. (1995) Multidimensional NMR in Lipid Systems. Coherence Transfer Through *J* Couplings Under MAS, *J. Magn. Reson. Ser. B* 106:187-190.

[4] Maas W. E., Laukien F. H., Cory D. G. (1996) Gradient, High Resolution, Magic Angle Sample Spinning NMR, *J. Am. Chem. Soc.* 118:13085-13086.

[5] Bruker BioSpin, (2012) Biological Tissue Analysis. Available: http://www.bruker-biospin.com/probes_hrmas.html. Accessed 2012 April 10.

[6] Agilent Technologies, (2012) Nano Probes. Available: http://www.chem.agilent.com/en-US/Products/Instruments/magneticresonance/nmr/probes/liquids/nano/pages/default.aspx. Accessed 2012 April 10.

[7] JEOL, (2012) FGMAS. Available: http://www.jeol.cn/?p=1232. Accessed 2012 April 10.

[8] Doty Scientific, (2012) HR-MAS MAG Probe. Available: http://www.dotynmr.com/solids/HRMASMAG.htm. Accessed 2012 April 10.

[9] Lindon J. C., Beckonert O. P., Holmes E., Nicholson J. K. (2009) High-Resolution Magic Angle Spinning NMR Spectroscopy: Application to Biomedical Studies, *Prog. Nucl. Mag. Res. Sp.* 55:79-100.

[10] Zietkowski D., Davidson R. L., Eykyn T. R., De Silva S. S., deSouza N. M., Payne G. S. (2010) Detection of Cancer in Cervical Tissue Biopsies Using Mobile Lipid Resonances

* Corresponding Author

Measured with Diffusion-Weighted ^{1}H Magnetic Resonance Spectroscopy, *NMR Biomed.* 23:382-390.

[11] Beckonert O., Coen M., Keun H. C., Wang Y., Ebbels T. M. D., Holmes E., Lindon J. C., Nicholson J. K. (2010) High-Resolution Magic-Angle-Spinning NMR Spectroscopy for Metabolic Profiling of Intact Tissues, *Nat. Protoc.* 5:1019-1032.

[12] Valentini M., Ritota M., Cafiero C., Cozzolino S., Leita L., Sequi P. (2011) The HRMAS-NMR Tool in Foodstuff Characterization, *Magn. Reson. Chem.* 49:S121-S125.

[13] Vermathen M., Marzorati M., Baumgartner D., Good C., Vermathen P. (2011) Investigation of Different Apple Cultivars by High Resolution Magic Angle Spinning NMR. A Feasibility Study, *J. Agric. Food Chem.* 59:12784-12793.

[14] Shapiro M. J., Gounarides J. S. (2001) High Resolution MAS-NMR in Combinatorial Chemistry, *Biotechnology Bioengineering (Combinatorial Chemistry)* 71:130-148.

[15] Power W. P. (2003) High Resolution Magic Angle Spinning - Applications to Solid Phase Synthetic Systems and Other Semi-Solids, *Annual Reports NMR Spectroscopy* 51:261-295.

[16] Shapiro M. J., Gounarides J. S. (1999) NMR Methods Utilized in Combinatorial Chemistry Research, *Progress Nuclear Magnetic Resonance* 35:153-200.

[17] Brown S. P. (2012) Applications of High-Resolution ^{1}H Solid-State NMR, *Solid State Nuclear Magnetic Resonance* 41:1-27.

[18] Schröder H. (2003) High Resolution Magic Angle Spinning NMR for Analyzing Small Molecules Attached to Solid Support, *Comb. Chem. High T. Scr.* 6:741-753.

[19] Thieme K., Zech G., Kunz H., Spiess H. W., Schnell I. (2002) Dipolar Recoupling in NOESY-Type ^{1}H-^{1}H NMR Experiments Under HRMAS Conditions, *Organic Letters* 4:1559-1562.

[20] Alam T. M., Holland g. P. (2006) ^{1}H-^{13}C INEPT MAS NMR Correlation Experiments with ^{1}H-^{1}H Mediated Magnetization Exchange to Probe Organization in Lipid Biomembranes, *J. Magn. Reson.* 180:210-221.

[21] Nicholls A. W., Mortishire-Smith R. J. (2001) Temperature Calibration of a High-Resolution Magic-Angle Spinning NMR Probe for Analysis of Tissue Samples, *Magn. Reson. Chem.* 39:773-776.

[22] Sodickson A., Cory D. G. (1997) Shimming a High-Resolution MAS Probe, *J. Magn. Reson.* 128:87-91.

[23] Engelke F., Maas W. E. (1997) *High Resolution Magic Angle Spinning Spectroscopy User Manual Version 1.0*: Bruker Instruments, Inc. 50 p.

[24] Piotto M., Elbayed K., Wieruszeski J. M., Lippens G. (2005) Practical Aspects of Shimming a High Resolution Magic Angle Spinning Probe, *J. Magn. Reson.* 173:84-89.

[25] Nishiyama Y., Tsutsumi Y., Utsumi H. (2012) MAGIC SHIMMING: Gradient Shimming with Magic Angle Sample Shimming, *J. Magn. Reson.* 216:197-200.

[26] Smallcombe S. H., Patt S. L., Keifer P. A. (1995) WET Solvent Suppression and Its Applications to LC NMR and High-Resolution NMR Spectroscopy, *J. Magn. Reson., A* 117:295-303.

[27] Warrass R., Wieruszeski J.-M., Lippens G. (1999) Efficient Suppression of Solvent Resonances in HR-MAS of Resin-Supported Molecules, *J. Am. Chem. Soc.* 121:3787-3788.

[28] Ng Y.-F., Meillon J.-C., Ryan T., Dominey A. P., Davis A. P., Sanders J. K. M. (2001) Gel-Phase MAS NMR Spectroscopy of a Polymer-Supported Pseudorotaxane and Rotaxane: Receptor Binding to an "Inert" Polyethylene Glycol Spacer, *Angew. Chem. Int. Ed.* 40:1759-1760.

[29] de Miguel Y. R., Bampos N., de Silva K. M. N., Richards S. A., Sanders J. K. M. (1998) Gel Phase MAS ^{1}H NMR as a Probe for Supramolecular Interactionas the Solid-Liquid Interface, *Chem. Commun.* 2267-2268.

[30] Hulst R., Seyger R. M., van Duynhoven J. P. M., van der Does L., Noordermeer J. W. M., Bantjes A. (1999) Vulcanization of Butadiene Rubber by Means of Cyclic Disulfides. 3. A 2D Solid State HRMAS NMR Study on Accelerated Sulrfur Vulcanizates of BR Rubber, *Macromolecules* 32:7521-7529.

[31] Hulst R., Seyger R. M., Van Duynhoven J. P. M., van der Does L., Noordermeer J. W. M., Bantjes A. (1999) Vulcanization of Butadiene Rubber by Means of Cyclic Disulfides. 2. A 2D Solid State HRMAS NMR Study of Cross-Link Structures in BR Vulcanizates, *Macromolecules* 32:7509-7520.

[32] Calucci L., Forte C., Ranucci E. (2007) Water/Polymer Interactions in a Poly(amidoamine) Hydrogel Studied by NMR Spectroscopy, *Biomacromolecules* 8:2936-2942.

[33] Annunziata R., Tranchini J., Ranucci E., Ferruti P. (2007) Structural Characterisation of Poly(Amidoamine) Networks Via High-Resolution Magic Angle Spinning NMR, *Magn. Reson. Chem.* 45:51-58.

[34] Sacristán M., Ronda J. C., Cádiz V. (2009) Silicon-Containing Soybean-Oil-Based Copolymers. Synthesis and Properties, *Biomacromolecules* 10:2678-2685.

[35] Van Camp W., Dispinar T., Dervaux B., Du Prez F. E., Martins J. C., Frtizinger B. (2009) 'Click' Functionalization of Cryogels Conveniently Verified and Quantified Using High-Resolution MAS NMR Spectroscopy, *Macromolecular Rapid Communications* 30:1328-1333.

[36] Crini G., Bourdonneau M., Martel B., Piotto M., Morcellet M., Richert T., Vebrel J., Torri G., Morin N. (2000) Solid-State NMR Characterization of Cyclomaltoheptoase (β-Cyclodextrin) Polymers Using High-Resolution Magic Angle Spinning with Gradients, *J. Applied Polymer Science* 75:1288-1295.

[37] Komber H., Ziemer A., Voit B. (2002) Etherification as Side Reactions in the Hyperbranched Polycondensationof 2,2-Bis(hydroxymethyl)propionic Acid, *Macromolecules* 35:3514-3519.

[38] Favier I., Gómez M., Muller G., Picurelli D., Nowicki A., Roucoux A., Bou J. (2007) Synthesis of New Functionalized Polymers and their use as Stabilizers of Pd, Pt, and Rh Nanoparticles. Preliminary Catalytic Studies, *J. Applied Polymer Science* 105:2772-2782.

[39] Bachmann S., Hellriegel C., Wegmann J., Händel H., Albert K. (2000) Characterization of Polyalkylvinyl Ether Phases by Solid-State and Suspended-State Nuclear Magnetic Resonance Investigations, *Solid State Nuclear Magnetic Resonance* 17:39-51.

[40] Schauff S., Friebolin V., Grynbaum M. D., Meyer C., Albert K. (2007) Monitoring the Interactions of Tocopherol Homologues with Reversed-Phase Stationary HPLC Phases by ^{1}H Suspended-State Saturation Transfer Difference High-Resolution Magic Angle Spinning NMR Spectroscopy, *Anal. Chem.* 79:8323-8326.

[41] Courtois J., Fischer G., Schauff S., Albert K., Irgum K. (2006) Interactions of Bupivacaine with a Molecularly Imprinted Polymer in a Monolithic Format Studied by NMR, *Anal. Chem.* 78:580-584.

[42] Melchels F. P. W., Velders A. H., Feijen J., Grijpma D. W. (2010) Photo-Cross Linked Poly(DL-Lactide)-Based Networks. Structural Characterization by HR-MAS NMR Spectroscopy and Hydrolytic Degradation Behavior, *Macromolecules* 43:8570-8579.

[43] Feng Y., Billon L., Grassl B., Khoukh A., Francois J. (2002) Hydrophobically Associated Polyacrylamides and their Partially Hydrolyzed Derivatives Prepared by Post-Modification. 1. Synthesis and Characterization, *Polymer* 43:2055-2064.

[44] Busico V., Causà M., Cipullo R., Credendino R., Cutillo F., Friederichs N., Lamanna R., Serge A., Castelli V. V. A. (2008) Periodic DFT and High-Resolution Magic-Angle-Spinning (HR-MAS) ^{1}H NMR Investigation of the Active Surfaces of $MgCl_2$-Supported Ziegler-Natta Catalysts. the $MgCl_2$ Matrix., *J. Phys. Chem. C* 112:1081-1089.

[45] Linder E., Brugger S., Steinbrecher S., Plies E., Mayer H. A. (2001) Investigations on the Mobility of Novel Sol-Gel Processed Inorganic-Organic Hybrid Materials, *J. Mater. Chem.* 11:1393-1401.

[46] Brenna S., Posset T., Furrer J., Blümel J. (2006) ^{14}N NMR and Two-Dimensional Suspension ^{1}H and ^{13}C HRMAS NMR Spectrscopy of Ionic Liquids Immobilized on Silica, *Chem. Eur. J.* 12:2880-2888.

[47] Rencurosi A., Lay L., Russo G., Prosperi D., Poletti L., Caneva E. (2007) HRMAS NMR Analysis in Neat Ionic Liquids: A Powerful Tool to Investigate Complex Organic Molecules and Monitor Chemical Reactions, *Green Chemistry* 9:216-218.

[48] Carvalho P. J., Álvarez V. H., Schröder B., Gil A. M., Marrucho I. M., Aznar M., Santos L. M. N. B. F., Coutinho J. A. P. (2009) Specific Solvation Interaction of CO_2 on Acetate and Trifluoroacetate Imidazolium Based Ionic Liquids at High Pressures, *J. Phys. Chem. B* 113:6803-6812.

[49] Lungwitz R., Spange S. (2008) Structure and Polarity of the Phase Boundry of *N*-Methylimidazolium Chloride/Silica, *J. Phys. Chem. C* 112:19443-19448.

[50] Le Bideau J., Gaveau P., Bellayer S., Néouze M.-A., Vioux A. (2007) Effect of Confinement on Ionic Liquids Dynamics in Monolithic Silica Ionogels: ^{1}H NMR Study, *Phys. Chem. Chem. Phys.* 9:5419-5422.

[51] Romanova E. E., Grinberg F., Pampel A., Kärger J., Freude D. (2009) Diffusion Studies in Confined Nematic Liquid Crystals by MAS PFG NMR, *J. Magn. Reson.* 196:110-114.

[52] Alam T. M., Dreyer D. R., Bielwaski C. W., Ruoff R. S. (2011) Measuring Molecular Dynamics and Activation Energies for Quanternary Acyclic Ammonium and Cyclic Pyrrolidinium Ionic Liquids using ^{14}N NMR Spectroscopy, *J. Phys. Chem. A* 115:4307-4316.

[53] Huster D., Gawrisch K. (1999) NOESY NMR Crosspeaks Between Lipid Headgroups and Hydrocarbon Chains: Spin Diffusion or Molecular Disorder?, *J. Am. Chem. Soc.* 121:1992-1993.

[54] Huster D., Arnold K., Gawrisch K. (1999) Investigation of Lipid Organization in Biological Membranes by Two-Dimensional Nuclear Overhauser Enhancement Spectroscopy *J. Phys. Chem. B* 103:243-251.

[55] Zhou H., Du F., Li X., Zhang B., Li W., Yan B. (2008) Characterization of Organic Molecules Attached to Gold Nanoparticle Surface Using High Resolution Magic Angle Spinning ^{1}H NMR, *J. Phys. Chem. C* 112:19360-19366.

[56] Krpetic Z., Scarì G., Caneva E., Speranza G., Porta F. (2009) Gold Nanoparticles Prepared Using Cape Aloe Active Compounds, *Langmuir Lett.* 25:7217-7221.

[57] Krpetic Z., Nativo P., Porta F., Brust M. (2009) A Multidentate Peptide for Stabilization of Facile Bioconjugation of Gold Nanoparticles, *Bioconjugate Chem.* 20:619-624.

[58] Polito L., Colombo M., Monti D., Melato S., Caneva E., Prosperi D. (2008) Resolving the Structure of Ligands Bound to the Surface of Superparamagnetic Iron Oxide Nanoparticles by High-Resolution Magic-Angle Spinning NMR Spectroscopy, *J. Am. Chem. Soc.* 130:12712-12724.

[59] Polito L., Monti D., Caneva E., Delnevo E., Russo G., Prosperi D. (2008) One-Step Bioengineering of Magnetic Nanoparticles via a Surface Diazo Transfer/Azide–Alkyne Click Reaction Sequence, *Chem. Commun.* 621-623.

[60] Deshayes S., Maurizot V., Clochard M.-C., Berthelot T., Baudin C., Déléris G. (2010) Synthesis of Specific Nanoparticles for Targeting Tumor Angiogenesis Using Electron-Beam Irradiation, *Radiation Phys. Chem.* 79:208-213.

[61] Costantino L., Gandolfi F., Bossy-Nobs L., Tosi G., Gurny R., Rivasi F., Vandelli M. A., Forni F. (2006) Nanoparticulate Drug Carriers Based on Hybrid poly(D,L-Lactide-*co*-Glycolide)-Dendron Structures, *Biomaterials* 27:4635-4645.

[62] Conte P., Carotenuto G., Piccolo A., Perlo P., Nicolais L. (2007) NMR-Investigations of the Mechanism of Silver Mercaptide Themolysis in Amorphous Polystyrene, *J. Mater. Chem.* 17:201-205.

[63] Blümel J. (2008) Linkers and Catalysis Immobilized on Oxide Supports: New Insights by Solid-State NMR Spectroscopy, *Coordination Chemistry Reviews* 252:2410-2423.

[64] Posset T., Rominger F., Blümel J. (2005) Immobilization of Bisphosphinoamine Linkers on Silica: Identification of Previously Unrecongnized Byproducts vis ^{31}P CP/MAS and Suspension HR-MAS Studies, *Chem. Mater.* 17:586-595.

[65] Guenther J., Reibenspies J., Blümel J. (2011) Synthesis, Immobilization, MAS and HR-MAS NMR of a New Chelate Phosphine Linker System, and Catalysis by Rhodium Adducts Thereof, *Adv. Synth. Catal.* 353:443-460.

[66] Posset T., Guenther J., Pope J., Oeser T., Blümel J. (2011) Immobilized Sonogashira Catalyst Systems: New Insights by Multinuclear HRMAS NMR Studies, *Chem. Commun.* 2011:2059-2061.

[67] Blümel J. (2008) Linkers and Catalysts Immobilized in Oxide Supports: New Insights by Solid-State NMR Spectroscopy, *Coordination Chemistry Reviews* 252:2410-2423.

[68] Pinoie V., Poelmans K., Miltner H. E., Verbruggen I., Biesemans M., Van Assche G., Van Mele B., Martins J. C., Willem R. (2007) A Polystyrene-Supported Tin Trichloride Catalyst with a C11-Spacer. Catalysis Monitoring Using High-Resolution Magic Angle Spinning NMR, *Organometallics* 26:6718-6725.

[69] Poelmans K., Pinoie V., Verbruggen I., Biesemans M., Deshayes G., Duquesne E., Delcourt C., Degée P., Miltner H. E., Dubois P., Willem R. (2008) Undecyltin Trichloride Grafted onto Cross-Linked Polystyrene: An Effecient Catalyst for Ring-Opening Polymerization of ε-Caprolactone, *Organometallics* 27:1841-1849.

[70] Deshayes G., Poelmans K., Verbruggen I., Camacho-Camacho C., Degée P., Pinoie V., Martins J. C., Piotto M., Biesemans M., Willem R., Dubois P. (2005) Polystyrene-Supported Organotin Dichloride as a Recyclable Catalyst in Lactone Ring-Opening Polymerization: Assessment and Catalysis Monitoring by High-Resolution Magic-Angle-Spinning NMR Spectroscopy, *Chem. Eur. J.* 11:4552-4561.

[71] Pinoie V., Biesemans M., Willem R. (2008) Quantitative Tin Loading Determination of Supported Catalysts by ^{119}Sn HRMAS NMR using a Calibrated Internal Signal (ERETIC), *Organometallics* 27:3633-3634.

[72] Porto S., Seco J. M., Espinosa J. F., Quiñoá E., Riguera R. (2008) Resin-Bound Chiral Derivatizing Agents for Assignments of Configuration by NMR Spectroscopy, *J. Organic Chem.* 73:5714-5722.

[73] Hellriegel C., Skogsberg U., Albert K., Lämmerhofer M., Maier N. M., Linder W. (2004) Characterization of a Chiral Stationary Phase by HR-MAS NMR Spectroscopy and Investigation of Enatioselective Interaction with Chiral Ligates by Transferred NOE, *J. Am. Chem. Soc.* 126:3809-3816.

[74] Simpson A. J., Kingery W. L., Sahw D. R., Spraul M., Humpfer E., Dvorstak P. (2001) The Application of ^{1}H HR-MAS NMR Spectroscopy for the Study of Structures and Associations of Organic Components at the Solid-Aqueous Interface of a Whole Soil., *Environ. Sci. Technol.* 35:3321-3325.

[75] Simpson A. J., Simpson M., Smith E., Kelleher B. P. (2007) Microbially Derived Input to Soil Organic Matter; Are Current Estimates Too Low?, *Environ. Sci. Technol.* 41:8070-8076.

[76] Feng X., Simpson A. J., Simpson M. (2006) Investigating the Role of Mineral-Bound Humic Acid in Phenanthrene Sorption, *Environ. Sci. Technol.* 40:3260-3266.

[77] Shirzadi A., Simpson M. J., Kumar R., Baer A. J., Xu Y., Simpson A. J. (2008) Molecular Interactions of Pestisides at the Soil-Water Interface, *Environ. Sci. Technol.* 42:5514-5520.

[78] Combourieu B., Inacio J., Delort A.-M., Forando C. (2001) Differentation of Mobile and Immobile Pesticides on Anionic Clays by ^{1}H HR MAS NMR Spectroscopy, *Chem. Commun.* 2214-2215.

[79] Colnago L. A., Martin-Neto L., Pérez M. G., Daolio C., Ferreira A. G., Camargo O. A., Berton R., Bettiol W. (2003) Application of ^{1}H HR/MAS NMR to Soil Organic Matter Studies, *Ann. Magn. Reson.* 2:116-118.

[80] Simpson A. J., Simpson M., Kingery W. L., Lefebvre B. A., Moser A., Williams A. J., Kvasha M., Kelleher B. P. (2006) The Application of ^{1}H High-Resolution Magic-Angle

Spinning NMR for the Study of Clay-Organic Associations in Natural and Synthetic Complexes, *Langmuir* 22:4498-4503.

[81] Simpson A. J., Kingery W. L., Hatcher P. G. (2003) The Indentification of Plant Derived Structures in Humic Materials Using Three-Dimensional NMR Spectroscopy, *Environ. Sci. Technol.* 37:337-342.

[82] Pampel A., Zick K., Glauner H., Engelke F. (2004) Studying Lateral Diffusion in Lipid Bilayers by Combining a Magic Angle Spinning NMR Probe with a Microimaging Gradient System, *J. Am. Chem. Soc.* 126:9534-9535.

[83] Stejskal E. O., Tanner J. E. (1965) Spin Diffusion Measurements: Spin Echoes in the Presence of Time-Dependent Field Gradient, *J. Chem. Phys.* 42:288-292.

[84] Viel S., Ziarelli F., Pagès G., Carrara C., Caldarelli S. (2008) Pulsed Field Gradient Magic Angle Spinning NMR Self-Diffusion Measurements in Liquids, *J. Magn. Reson.* 190:113-123.

[85] Cotts R. M., Hoch M. J. R., Sun T., Marker J. T. (1989) Pulsed Field Gradient Stimulated Echo Methods for Improved NMR Diffusion Measurements in Heterogeneous Systems, *J. Magn. Reson.* 83:252-266.

[86] Tanner J. E. (1970) Use of the Stimulated Echo in NMR Diffusion Studies, *J. Chem. Phys.* 52:2523-2526.

[87] Gibbs S. J., Johnson Jr. C. S. (1991) A PFG NMR Experiment for Accurate Diffusion and Flow Studies in the Presence of Eddy Currents, *J. Magn. Reson.* 93:395-402.

[88] Pampel A., Fernandez M., Freude D., Kärger J. (2005) New Options for Measuring Molecular Diffusion in Zeolites by MAS PFG NMR, *Chem. Phys. Lett.* 407:53-57.

[89] Pampel A., Engelke F., Galvosas P., Krause C., Stallmach F., Michel D., Kärger J. (2006) Selective Multi-Component Diffusion Measurement in Zeolites by Pulsed Field Gradient NMR, *Micropor. Mesopor. Mat.* 90:271-277.

[90] Fernandez M., Pampel A., Takahashi R., Sato S., Freude D., Kärger J. (2008) Revealing Complex Formation in Acetone-*n*-Alkane Mixtures by MAS PFG NMR Diffusion Measurement in Nanoporous Hosts, *Phys. Chem. Chem. Phys.* 10:4165-4171.

[91] Fernandez M., Kärger J., Freude D., Pampel A., van Baten J. M., Krishna R. (2007) Mixture Diffusion in Zeolites Studied by MAS PFG NMR and Molecular Simulation, *Micropor. Mesopor. Mat.* 105:124-131.

[92] Gaede H. C., Gawrisch K. (2003) Lateral Diffusion Rates of Lipid, Water and a Hydrophobic Drug in a Multilamellar Liposome, *Biophys. J.* 85:1734-1740.

[93] Gaede H. C., Gawrisch K. (2004) Multi-Dimensional Pulse Field Gradient Magic Angle Spinning NMR Experiments on Membranes, *Magn. Reson. Chem.* 42: 115-122.

[94] Polozov I. V., Gawrisch K. (2004) Domains in Binary SOPC/POPE Lipid Mixtures Studied by Pulsed Field Gradient ^{1}H MAS NMR, *Biophys. J.* 87:1741-1751.

[95] Iqbal S., Rodríguez-Lansola F., Escuder B., Miravet J. F., Verbruggen I., Willem R. (2010) HRMAS ^{1}H NMR as a Tool for the Study of Supramolecular Gels, *Soft Matter* 6:1875-1878.

[96] Chin J. A., Chen A., Shapiro M. J. (2000) SPEEDY: Spin-Echo Enhanced Diffusion Filtered Spectroscopy. A New Tool for High Resolution MAS NMR, *J. Comb. Chem.* 2:293-296.